

## Distinctive compartmental organization of human primary visual cortex

TODD M. PREUSS\*<sup>†</sup>, HUIXIN QI<sup>‡</sup>, AND JON H. KAAS<sup>‡</sup>

\*Institute of Cognitive Science, University of Louisiana at Lafayette, 4401 West Admiral Doyle Drive, New Iberia, LA 70560; and <sup>‡</sup>Department of Psychology, Vanderbilt University, 301 Wilson Hall, Nashville, TN 37240

Communicated by Mortimer Mishkin, National Institutes of Health, Bethesda, MD, August 9, 1999 (received for review June 4, 1999)

**ABSTRACT** In the primary visual area of macaques and other monkeys, layer 4A is a mosaic of separate tissue compartments related to the parvocellular (P) and magnocellular (M) layers of the lateral geniculate nucleus. This mosaic resembles a honeycomb, with thin walls that receive direct P inputs and cores consisting of columns of dendrites and cell bodies ascending from layer 4B, a layer that receives indirect M inputs. To determine whether apes and humans have a macaque-like layer 4A, we examined the primary visual area in humans, chimpanzees, an orangutan, Old World monkeys, and New World monkeys. Apes and humans lacked the dense band of cytochrome oxidase staining in layer 4A that marks the stratum of P-geniculate afferents in monkeys. Furthermore, humans displayed a unique arrangement of presumed M-related cells and dendrites in layer 4A, as revealed with antibodies against nonphosphorylated neurofilaments and microtubule-associated protein 2. Human 4A contained a large amount of M-like tissue distributed in a complex, mesh-like pattern rather than in simple vertical arrays as in other anthropoid primates. Our results suggest that (i) the direct P-geniculate projection to layer 4A was reduced early in the evolution of the ape–human group, (ii) the M component of layer 4A was subsequently modified (and possibly enhanced) in the human lineage, and (iii) the honeycomb model does not adequately characterize human layer 4A. This is the first demonstration of a difference in the cortical architecture of humans and apes, the animals most closely related to humans.

Our current understanding of the structure and function of the human visual system depends critically on experimental studies of nonhuman primates, especially macaque monkeys. The emphasis on macaques is justified by the fact that the visual systems of macaques and humans share many similarities (e.g., refs. 1–7). There is, however, growing evidence that humans also differ from macaques in some aspects of visual organization. For instance, the parasol retinal ganglion cells of humans have much larger dendritic fields than those of macaques, although the dendrites of human and macaque midget cells are of similar size (8). Because parasol cells project to the magnocellular (M) layers of the lateral geniculate nucleus (LGN), it is reasonable to expect that there are macaque–human differences in aspects of visual function mediated by the M stream, such as sensitivity to motion and to luminance contrast. There are, in fact, reports that humans are more sensitive than macaques to spatial and temporal luminance contrast under photopic conditions (9, 10).

In addition to evidence for M-stream differences, there are indications that humans differ from nonhuman primates in the organization of the visual pathway that involves the parvocellular (P) layers of the LGN. Studies of connectivity (reviewed

in refs. 11 and 12) indicate that, in Old World and New World monkeys, the P geniculate layers send a projection to layer 4A of the primary visual area (area V1), separate from the larger projection that targets the deep part of layer 4C (4C $\beta$ ). The P projection to 4A is coincident with a band of dense cytochrome oxidase (CO) staining separate from the thick, densely stained band that marks layer 4C (13). However, layer 4A has inputs from the M-stream as well as from the P stream. The M-LGN layers project to layer 4C $\alpha$ , which in turn projects to layer 4B, and the apical dendrites of layer 4B pyramidal cells form bundles that pass upward through layer 4A, accompanied by a number of pyramidal cell somas (14–16). These prominent dendrites can be revealed with antibodies that recognize microtubule-associated protein 2 (MAP 2) (14–16) and non-phosphorylated neurofilaments (NPNF) (17). Thus, as summarized in Fig. 1, layer 4A of macaques is a mosaic of separate tissue compartments related to the P and M streams, organized like a honeycomb (14–18).

The honeycomb model has wide applicability in anthropoid primates: Among taxa that have been studied—which include at least five genera of New World monkeys (13, 19–21) and four genera of Old World monkeys (13, 22, 23)—only the nocturnal owl monkey (*Aotus* spp.) lacks a direct P-LGN connection to layer 4A and a corresponding CO-dense band (13). The fact that the honeycomb is so common in New World and Old World monkeys suggests it should be present in hominoid primates (apes and humans), animals that are closely related to Old World monkeys (24). It is thus surprising that published studies are unanimous in reporting that humans lack a CO-dense 4A band (17, 25–28). This finding has led Wong-Riley *et al.* (28) to suggest that the organization of the geniculate projection to layer 4A may have been modified in humans compared with monkeys. However, Wong-Riley (28) also raises the possibility that the difference in CO staining is an artifact of relatively poor tissue preservation in humans compared with monkeys: Experimental monkey tissue is typically fixed by perfusion at the time of death whereas in humans, brains are removed several hours after death and are fixed by immersion in aldehydes, and the delay could result in loss of CO activity.

The possibility that the organization of the primary visual area differs in humans and macaques has prompted relatively little discussion. One reason for this may be the suspicion that the reported difference in CO activity is artifactual. Moreover, even if there is a difference in CO activity, there need not be a major difference in area V1 organization: In macaques, layer 4A receives indirect inputs from the P stream via a projection from layer 4C $\beta$  (29) in addition to the direct inputs from the P geniculate layers, so a reduction or loss of the direct P geniculate input in humans might have relatively minor func-

The publication costs of this article were defrayed in part by page charge payment. This article must therefore be hereby marked “advertisement” in accordance with 18 U.S.C. §1734 solely to indicate this fact.

PNAS is available online at [www.pnas.org](http://www.pnas.org).

Abbreviations: CO, cytochrome oxidase; LGN, lateral geniculate nucleus; NPNF, nonphosphorylated neurofilament protein; M, magnocellular; MAP 2, microtubule-associated protein 2; P, parvocellular; area V1, primary visual area.

<sup>†</sup>To whom reprint requests should be addressed. E-mail: [tmp8292@usl.edu](mailto:tmp8292@usl.edu).

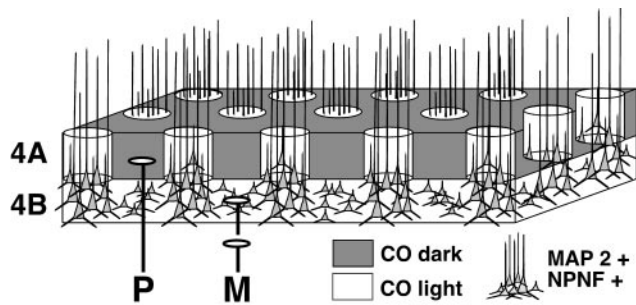


FIG. 1. The honeycomb model of layer 4A organization, as derived from studies of macaques and other monkeys. Layer 4A consists of a sheet of tissue that receives direct inputs from the P layers of the LGN and that stains darkly for CO. The sheet is punctuated by clusters of apical dendrites and pyramidal cell somas extending upward from layer 4B. Layer 4B receives indirect input from the M layers of the LGN. Cells and dendrites in layer 4B and related portions of 4A stain densely for MAP 2 and NPNF.

tional consequences. Finally, empirical support for a human honeycomb has been offered by Yoshioka and Hendry (17), who labeled the M-related components of human layer 4A by staining for NPNF with the SMI-32 antibody (30, 31). Yoshioka and Hendry argued that NPNF staining in humans revealed cores of darkly stained, M-like dendrites and cell bodies surrounded by a lattice of unstained, presumably P-like territories, consistent with the honeycomb model. Yoshioka and Hendry did not, however, directly compare human and nonhuman patterns of NPNF immunostaining, and, furthermore, they reported finding little immunostaining for MAP 2 in human area V1, in contrast to results in macaques (14–16).

The present study was carried out to clarify the similarities and differences in the organization of area V1 in humans and other primates. One specific goal was to determine whether the unusual laminar distribution of CO staining reported in humans is unique to humans or whether it is also present in apes, the animals most closely related to humans. To this end, we stained for CO in humans, apes, Old World monkeys, and New World monkeys. These investigations used both perfused and unperfused ape and monkey tissue and thus bear on the question of whether CO staining in humans is affected by different fixation conditions. A second goal was to directly compare the organization of the presumed M-related elements of layer 4A in humans and other primates by immunostaining for NPNF and MAP 2. It is noteworthy that this is one of the very few modern studies to directly compare the cerebral histology of humans and apes, notwithstanding their close evolutionary relationship (see also ref. 32).

## MATERIALS AND METHODS

**Subjects and Tissue Preparation.** We examined the occipital lobes of five humans (*Homo sapiens*), nine common chimpanzees (*Pan troglodytes*), one orangutan (*Pongo pygmaeus*), six Old World macaque monkeys (representing *Macaca mulatta*, *Macaca nemestrina*, *Macaca fascicularis*, and *Macaca assamensis*), four Old World vervet monkeys (*Cercopithecus aethiops*), four New World squirrel monkeys (*Saimiri sciureus*), and three New World spider monkeys (*Ateles geoffroyi*). Human tissue was acquired from the Northwestern University Alzheimer's Disease Center. The individuals were adults of both sexes ranging in age from 54 to 83 years (mean = 68). Four of five brains were rated as normal controls on neuropathological criteria by the Northwestern University Alzheimer's Disease Center. Postmortem intervals ranged from 3 to 18 hours. The orangutan brain and three of the chimpanzee brains came from individuals from the New Iberia Research Center that died of natural causes and had no known neurological or behavioral

abnormalities. Postmortem intervals ranged from 2 to 12 hours. A fourth chimpanzee brain came from an animal euthanized for veterinary reasons at the Yerkes Primate Center of Emory University but was sectioned and stained at the University of Louisiana at Lafayette. Five additional chimpanzees were euthanized for veterinary reasons at the Yerkes Primate Center, and their brains were processed at Yerkes by Drs. Johannes and Margarete Tigges. The chimpanzee individuals were adults, ranging from 16 to over 50 years of age. The monkey brains came from the University of Louisiana at Lafayette's New Iberia Research Center and Vanderbilt University animals. All procedures involving non-human species were carried out in accordance with institutional animal welfare guidelines.

Humans brains were removed from the skull, were blocked in the coronal plane in thin (1–1.5 cm thick) slabs to reduce fixation artifact, and were immersed in phosphate-buffered 4% paraformaldehyde for 24–95 hours. One chimpanzee brain and the orangutan brain were prepared in comparable manner. Two other chimpanzee brains were immersed whole or in large blocks in buffered 10% formalin or 4% paraformaldehyde for 3 days in one case and 40 days in the second. A fourth chimpanzee was fixed by perfusion with 4% paraformaldehyde and was postfixed for 24 hours in 2% paraformaldehyde. The five chimpanzees prepared at Yerkes were perfused with a mixture of 4% paraformaldehyde and 0.1% glutaraldehyde. The majority of Old World and New World monkeys were fixed by perfusion with 2–4% paraformaldehyde or with a mixture of 2–4% paraformaldehyde and 0.08–0.15% glutaraldehyde. However, four macaques were fixed by immersion in 2–4% paraformaldehyde for 4–9 days after postmortem intervals of 10 minutes to 5 hours. Brain blocks were subsequently cryoprotected with sucrose or glycerol solutions and were cut on freezing microtomes at 40–50  $\mu$ m in standard planes (in most cases the coronal plane). Sections were collected in phosphate buffer, transferred to cryoprotectant solution, and then stored at  $-20^{\circ}\text{C}$  before histological processing.

**Histochemistry.** Sections from five *Homo*, nine *Pan*, one *Pongo*, five *Macaca*, four *Cercopithecus*, two *Saimiri*, and three *Ateles* were reacted for cytochrome oxidase (33). In most cases, the reaction product was enhanced with cobalt chloride or imidazole (34). Immunostaining for NPNF and MAP 2 was carried out using standard streptavidin-biotin and diaminobenzidine techniques (35). The diaminobenzidine reaction was intensified by using imidazole or (in a few cases) nickel and cobalt. Sections were pretreated with methanol and hydrogen peroxide to enhance membrane permeability and to inactivate endogenous peroxidase. To further facilitate penetration of the immunoreagents, Triton X-100 was used in both the blocking and primary antibody incubation steps, typically at a concentration of 0.1%. In all cases, control sections were run that were not exposed to the primary antibody, which resulted in the absence of specific staining. We stained for NPNF by using monoclonal antibody SMI-32 (Sternberger Monoclonals, Baltimore) at a 1:2,000 dilution in five *Homo*, four *Pan*, one *Pongo*, five *Macaca*, three *Cercopithecus*, four *Saimiri*, and two *Ateles*. We stained for MAP 2 by using clone HM-2 (Sigma) at dilutions of 1:8,000 or 1:10,000 in five *Homo*, three *Pan*, one *Pongo*, four *Macaca*, three *Cercopithecus*, four *Saimiri*, and two *Ateles*.

**Analysis.** The laminar distribution of CO and immunostaining was assessed by examining Nissl-counterstained sections or neighboring sections stained for Nissl only. Digital images of stained sections were acquired with a Diagnostic Instruments (Sterling Heights, MI) Spot camera. ADOBE PHOTOSHOP software (Adobe Systems, Mountain View, CA) was used to adjust illumination levels and sharpen images. We also used PHOTOSHOP's tools for splitting color channels to evaluate the laminar organization of diaminobenzidine labeling in Nissl-counter-

stained sections, separating the red-brown diaminobenzidine-imidazole-stained elements from the blue Nissl-stained elements.

We identified the layers of area V1 according to the system of Brodmann (36), as modified by Lund (37). This system distinguishes four subdivisions of layer 4, namely, 4A, 4B, 4C $\alpha$ , and 4C $\beta$ . There are good reasons to regard layers "4A" and "4B" as subdivisions of layer 3, rather than layer 4 (11, 38), but we used the Brodmann-Lund system here because it has been so widely used in modern studies of primate visual cortex.

The inferences about patterns of evolutionary change offered in this study presuppose that the relationships among living anthropoid primate groups are well understood. This is the case (24), although it remains controversial whether gorillas are more distantly related to humans than are chimpanzees (39). The outcome of this debate does not affect the present analysis.

## RESULTS

Our results confirm that the CO staining pattern of humans differs from that of monkeys and also indicate that at least some ape species display a human-like pattern (Fig. 2). Both apes and humans (Fig. 2 *D-F*) lack a dark-staining layer 4A band, and both possess a band of moderate staining in layer 4B that is not typically present in monkeys (Fig. 2 *A-C*). It is unlikely, furthermore, that the absence of a 4A band in hominoids is artifactual: The band was absent from ape brains regardless of whether they were fixed by perfusion or immersion, and it was present in immersion-fixed macaques brains as well as those that were perfused (compare Fig. 2 *C* and *E*).

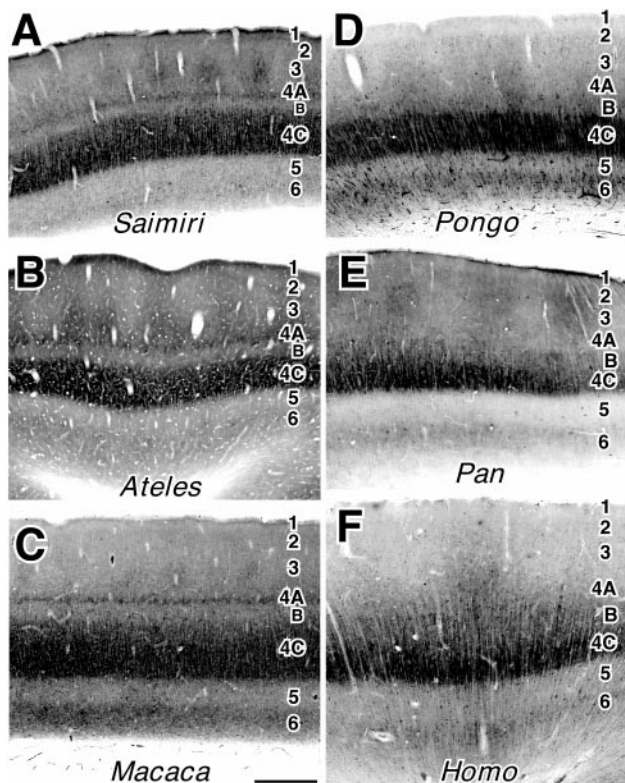


FIG. 2. Cytochrome oxidase staining of area V1 in the New World monkeys *Saimiri* (*A*) and *Ateles* (*B*), the Old World monkey *Macaca* (*C*), and the hominoids *Pongo* (*D*), *Pan* (*E*), and *Homo* (*F*). A CO-dense band is present in layer 4A in all of the monkeys, even those that were immersion fixed (as in *C*), but is absent in all of the hominoids, including perfusion-fixed chimpanzees (as in *E*). (Bar = 500  $\mu\text{m}$ .)

As with CO staining, immunostaining for NPNF revealed both similarities and differences across species (Fig. 3). All species exhibited dark bands composed of labeled cell bodies and neuropil in layers 6 and 4B and somewhat lighter staining in layers 5 and 4C $\alpha$ . One especially striking difference was evident in the upper cortical layers. In apes and humans, layer 3 was densely packed with stained pyramidal cell bodies and neuropil, and stained apical dendrites extended into layer 2 (Fig. 3 *D-I*) whereas in the monkeys, layer 3 staining was either much weaker (Fig. 3 *B* and *C*) or more narrowly restricted (Fig. 3 *A*). However, the difference in NPNF expression between hominoids and monkeys was not restricted to area V1 but, rather, extended over much of the neocortex (see also ref. 40). These results confirm and extend those of Campbell and Morrison (30), who reported that humans display much more

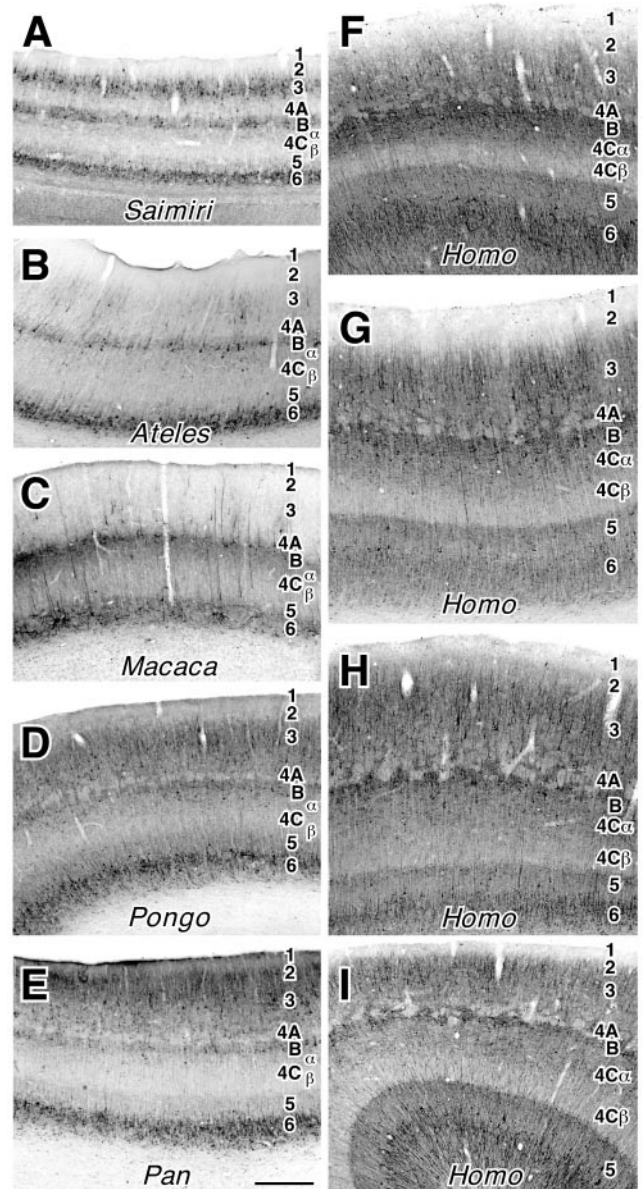


FIG. 3. Immunostaining for NPNF in *Saimiri* (*A*), *Ateles* (*B*), *Macaca* (*C*), *Pongo* (*D*), *Pan* (*E*), and four human individuals (*F-I*). Humans are distinguished from other primates by bands of dark-staining tissue that extend into layer 4A from layer 4B. These bands surround and cap small territories of lightly stained tissue in layer 4A, giving this layer a distinctive, mesh-like appearance. The dense and extensive NPNF immunoreactivity evident in layer 3 of apes (*D, E*) and humans (*F-I*) is a general characteristic of neocortex in these taxa, not a specific characteristic of area V1. (Bar = 500  $\mu\text{m}$ .)

extensive layer 3 NPNF staining than do macaques in area V1 and other parts of neocortex.

Humans exhibited an additional and distinctive feature of NPNF immunoreactivity that was not observed in other taxa. In New World and Old World monkeys, layer 4A appeared as a rather uniform light band, punctuated by vertically oriented dendrites and occasional cell bodies extending upward from the dark band of layer 4B (Fig. 3 A–C; Fig. 4A), consistent with the honeycomb model. In ape layer 4A, some prominent bands of NPNF-stained material could be seen to bridge the gap between layers 4B and 3 (Fig. 3 D and E). Nevertheless, as in monkeys, ape layer 4A stained rather lightly overall for NPNF, and those cells and neurites in layer 4A that stained for NPNF were predominantly vertically oriented (Fig. 4B). In contrast to monkeys and apes, human layer 4A had an extremely irregular appearance resulting from the extension of bands of dark-staining tissue from layer 4B into 4A, where they appeared to envelop and cap lightly stained territories (Fig. 3 F–I; Fig. 4C). As a result, human layer 4A had a characteristic mesh-like appearance. Within the bands of dark tissue coursing through layer 4A, we observed some remarkable arrangements of cells, with chains of tightly clustered somas and dendrites looping around pale zones (Fig. 4C). The pale zones demarcated by the dark bands adopted a variety of shapes and sizes, but they were typically round or somewhat oblong, and most measured between 60 and 120 microns in the plane parallel to the pial surface. The thickness of 4A could be spanned by a single large capsule or by clusters of two or more smaller capsules. In some cases, the fenestrated appearance of layer 4A appeared to extend into the deep part of layer 3 (Fig. 3 G and H). We observed this mesh-like pattern of 4A staining with NPNF in all of our human cases and in none of the other species we examined.

MAP 2 immunostaining was more variable in quality than NPNF staining, and some of our human and ape material in particular evinced rather weak staining. However, we obtained dense staining of neurites and cells bodies in three human cases and two ape cases, and the laminar distribution of staining in these cases generally resembled that observed in Old World

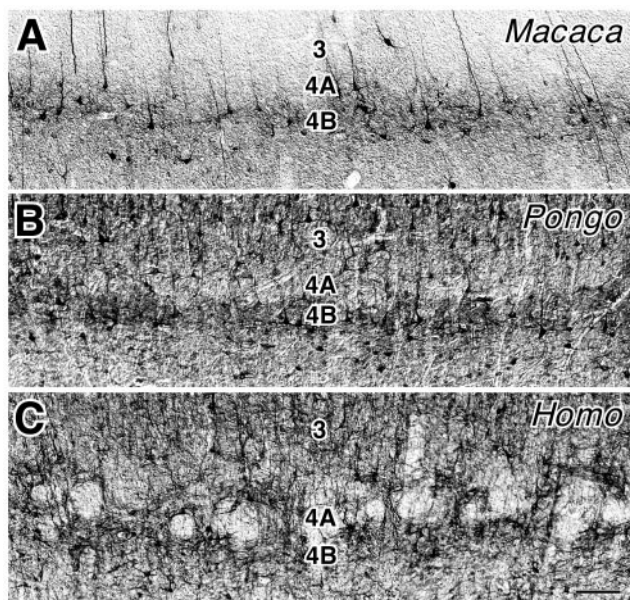


FIG. 4. NPNF immunostaining in layer 4A as seen with differential-interference contrast optics. In *Macaca* (A) and *Pongo* (B), layer 4A is generally lightly stained, although some vertically oriented dendrites and cell bodies are present that stain darkly for NPNF. By contrast, in *Homo* (C), layer 4A is laced with bands of dark, NPNF-immunoreactive tissue that encapsulate pockets of lightly stained tissue. (Bar = 100  $\mu\text{m}$ .)

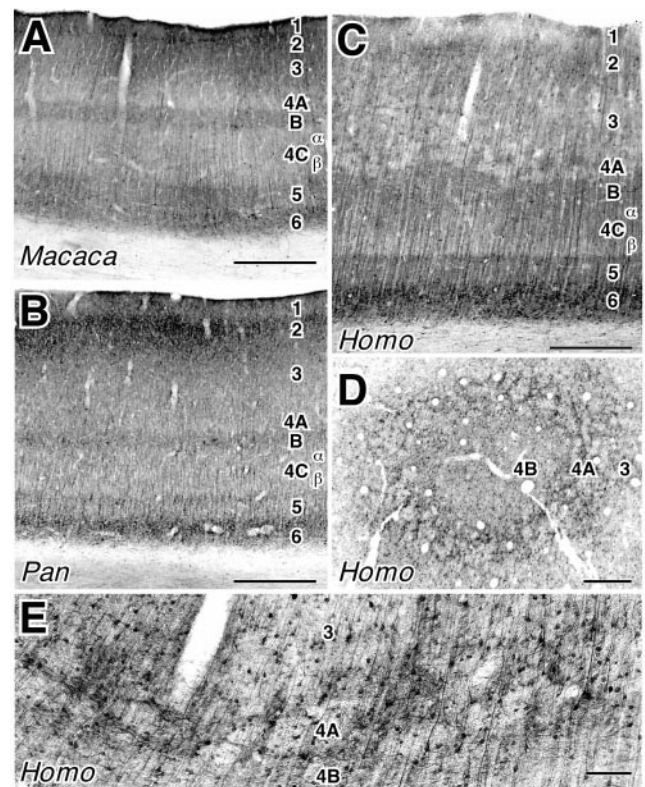


FIG. 5. MAP 2 immunostaining of area V1 in *Macaca* (A), *Pan* (B), and *Homo* (C–E). A–C are from standard coronal and horizontal sections. D is from a section that passes tangentially through the middle cortical layers in a human. E shows the organization of human layer 4A in the coronal plane with DIC optics. A distinctive, patchy, mesh-like pattern is apparent in layer 4A of humans in both coronal and tangential planes. [Bar = 500  $\mu\text{m}$  (A–D) and 100  $\mu\text{m}$  (E)].

and New World monkeys (Fig. 5 A–C). All of our well stained monkey, ape, and human cases exhibited dense immunoreactivity in layer 6, with lighter bands of immunostaining in layers 5 and 4B. Lighter staining was observed in layers 4C and deep layer 3 whereas the density of staining in upper layer 3 and layer 2 was quite variable across cases. Most significantly, however, in our three human cases that stained well for MAP 2, the appearance of layer 4A differed from that of apes and monkeys, displaying an irregular, fenestrated pattern similar to that observed in human tissue stained for NPNF (Fig. 5 C–E).

To date, we have not been able to obtain human brain material suitable for examining layer 4A in flattened sections. In one case, however, a portion of calcarine cortex was folded in such a way that coronal sections passed tangentially through layer 4A. This region exhibited a mesh-like pattern of staining for NPNF and MAP 2 (Fig. 5D), similar to that seen in coronal sections.

## Discussion

This study documents at least two differences in the organization of the primary visual area of humans compared with Old World and New World monkeys (Fig. 6). First, humans differ from monkeys in the laminar distribution of CO activity in layers 4A and 4B, a difference that may reflect evolutionary changes in the organization of P geniculate inputs to area V1. Moreover, CO staining in apes resembles that in humans. Second, humans differ from monkeys (and from apes) in the architecture of the presumed M-related elements of layer 4A, which stain for NPNF and MAP 2. It is very likely, therefore, that the compartmental organization of M- and P-related

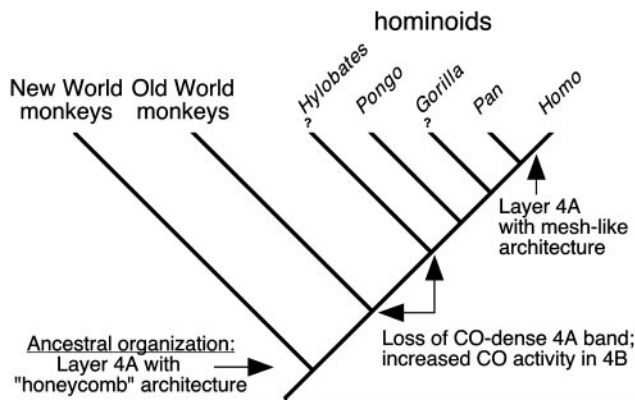


FIG. 6. An interpretation of changes in area V1 organization that took place during the evolutionary radiation of the hominoid primates (apes and humans). Changes are mapped onto a tree depicting the evolutionary relationships of primates (24).

territories within human layer 4A differs from the pattern described in monkeys.

Our results confirm previous reports that the CO staining pattern of humans differs from that of most monkeys (17, 25–28) and indicate that at least some apes, specifically, chimpanzees and probably also orangutans, possess a human-like condition. The ape–human pattern is marked by the absence of the thin, dense band of CO staining within layer 4A that is typical of nonhominoids, along with darker staining of layer 4B than is seen in monkeys. The enhanced CO staining of layer 4B in humans has not previously been described. Our results weigh against the possibility that the observed phyletic differences are artifacts of differential tissue preservation, as the staining patterns we observed in chimpanzees and macaques were qualitatively similar whether the animals were fixed by perfusion or by postmortem immersion.

The presence of dense CO staining in layer 4A and light staining in layer 4B in most New World and Old World monkeys that have been examined suggests that this was the ancestral pattern for anthropoid primates (Fig. 6). Consequently, the hominoid pattern of light staining in layer 4A and darker staining of 4B should be interpreted as a derived (specialized) characteristic. We currently lack information about CO activity in gibbons (genus *Hylobates*), which makes it impossible to determine whether the pattern of CO activity characteristic of humans, chimpanzees, and orangs evolved before or after the lineage leading to gibbons separated from the lineage leading to the other apes and humans. We also lack data about CO activity in gorillas, although we would expect these animals to resemble *Homo*, *Pan*, and *Pongo*.

The most significant result of the present study is the demonstration of a remarkable, mesh-like architectural pattern in human layer 4A (possibly extending into the deep part of layer 3) using antibodies against NPNF and MAP 2. Previous accounts of NPNF staining in humans did not report the distinctive pattern of staining reported here, although it can be discerned in some published photomicrographs (17, 30, 41). By contrast to our results in humans, the laminar distribution of NPNF and MAP 2 staining we observed in Old World and New World monkeys was similar to that described in earlier studies of these proteins in the Old World monkeys *Macaca* (14–16, 30, 42, 43) and *Cercopithecus* (44). Moreover, the fact that apes possess a rather monkey-like layer 4A, when stained for NPNF or MAP 2, suggests that the meshwork architecture is a true human evolutionary specialization, rather than a hominoid (ape–human) specialization.

The nature of the anatomical specializations of area V1 documented here point to possible differences in the way M and P inputs influence cortical visual processing in humans,

apes, and monkeys. The loss of dense CO staining in layer 4A of humans and apes suggest that P-geniculate projections to this layer, which are present in most monkeys, were reduced or lost in humans and apes. Alternatively, P-geniculate terminal fields might persist in humans and apes but have a more dispersed distribution than in monkeys, where they are confined to a narrow, compact band. There have been very few studies of geniculocortical connections in humans and apes, although the few reports that do exist are consistent with the absence of a projection to layer 4A in these species (45, 46). Additional investigations of ape and human geniculocortical connections are clearly warranted.

Our results also suggest strongly that the M-related components of layer 4A were modified in recent human evolution. The mesh-like architecture of humans reflects a change in the spatial arrangements of cell bodies and dendrites in layer 4A, such that bands of tissue that express NPNF and MAP 2 (presumably tissue with M affinities) came to envelop patches of lightly stained tissue (presumably territories with P affinities). As a result, humans are alone among primate species examined in having large amounts of NPNF- and MAP 2-immunoreactive tissue in layer 4A. These architectural changes suggest there were changes in information processing within the M pathway during human evolution, or in the manner in which the M and P streams interact within layer 4A (47), and possibly also an enhancement or augmentation of M representation in layer 4A. An augmentation of M representation in human area V1 would accord with reports that the M-related retinal ganglion cells of humans have larger dendritic field than those of macaques (8) and that humans are more sensitive to luminance contrast than are macaques (9, 10).

The identification of human specializations of M representation in area V1 has potentially important implications for our understanding of human visual function. Modifications of area V1 organization should be reflected at higher levels of the human visual system, as extrastriate cortex receives most of its visual information from area V1 (11, 48). It is therefore noteworthy that the extrastriate area known as V3A is very sensitive to moving stimuli in humans, unlike its macaque counterpart (49). Elucidation of human visual specializations might lead to a more complete understanding of developmental dyslexia, a disorder accompanied by pathology and dysfunction of the M system (50, 51).

This study also has important implications for the understanding of human brain evolution. As far as we can determine, the meshwork architecture of human layer 4A is the first documented feature of brain organization, not obviously related to differences in brain size, that distinguishes humans from apes, our closest relatives. This is perhaps not surprising, given the dearth of modern neuroscientific studies of apes. It is also the case, however, that classical discussions of human brain evolution neglected the possibility of changes in histology or connectivity (52–54), focusing instead on the dramatic increases in brain size that took place in the human lineage subsequent to the ape–human divergence and the concomitant expansion of higher-order association cortex (36, 55). The present results illustrate that human brain evolution entailed modification of neuronal architecture as well as changes in brain size. Furthermore, evolutionary modifications were not restricted to higher-order association cortex, but also involved sensory cortex—indeed, cortex situated at a very early stage in the visual-processing hierarchy (11, 48). Future investigations can be expected to reveal additional human specializations of neural organization and function. Candidate specializations include several reported human–monkey differences (56–59). As the present study illustrates, however (see also ref. 32), humans and apes can share brain characteristics not found in monkeys, and it is therefore necessary to compare humans and

apes to determine which human–monkey differences are true human specializations.

We thank Drs. Bruce Quinn, John Smiley, Margarete Tigges, and Johannes Tigges, and the veterinary staff of the New Iberia Research Center for assistance in acquiring brain material. Ghislaine Quessy-Coleman, Ryan Domingue, and Kyle Hebert provided expert histological support. This project was supported by the McDonnell-Pew Program in Cognitive Neuroscience (Grant JSMF 98-455), the National Institutes of Health (Grant EY 02686), the Institute of Cognitive Science, the New Iberia Research Center, and the Clinical Core of the Northwestern Alzheimer's Disease Center, Chicago, funded by National Institute on Aging Grant NS1P30 AG-13854-01 to Northwestern University.

1. Bradley, D. C., Chang, G. C. & Andersen, R. C. (1998) *Nature (London)* **392**, 714–717.
2. Cowey, A. & Stoerig, P. (1995) *Nature (London)* **373**, 247–249.
3. De Valois, R. L., Morgan, H. C., Polson, M. C., Mead, W. R. & Hull, E. M. (1974) *Vision Res.* **14**, 53–67.
4. Jacobs, G. H. & Deegan, J. F., II (1997) *Visual Neurosci.* **14**, 921–928.
5. Logothetis, N. K. & Schall, J. D. (1989) *Science* **245**, 761–763.
6. Newsome, W. T., Mikami, A. & Wurtz, R. H. (1986) *J. Neurophysiol.* **55**, 1340–1351.
7. Weiskrantz, L. (1972) *Proc. R. Soc. Lond. Ser. B* **182**, 427–455.
8. Dacey, D. M. & Petersen, M. R. (1992) *Proc. Natl. Acad. Sci. USA* **89**, 9666–9670.
9. De Valois, R. L., Morgan, H. C. & Snodderly, D. M. (1974) *Vision Res.* **14**, 75–81.
10. Merigan, W. H. (1980) *Vision Res.* **20**, 953–959.
11. Casagrande, V. A. & Kaas, J. H. (1994) in *Cerebral Cortex, Volume 10: Primary Visual Cortex in Primates*, eds. Peters, A. & Rockland, K. (Plenum, New York), pp. 201–259.
12. Wong-Riley, M. T. T. (1994) in *Cerebral Cortex, Volume 10: Primary Visual Cortex in Primates*, eds. Peters, A. & Rockland, K. (Plenum, New York), pp. 141–200.
13. Horton, J. C. (1984) *Philos. Trans. R. Soc. London B* **304**, 199–253.
14. Hendry, S. H. & Bhandari, M. A. (1992) *Visual Neurosci.* **9**, 445–459.
15. Peters, A. & Sethares, C. (1991) *J. Comp. Neurol.* **306**, 1–23.
16. Peters, A. & Sethares, C. (1991) *Cereb. Cortex* **1**, 445–462.
17. Yoshioka, T. & Hendry, S. H. C. (1995) *J. Comp. Neurol.* **359**, 213–220.
18. Hendrickson, A. E., Movshon, J. A., Eggers, H. M., Gizzi, M. S., Boothe, R. G. & Kiorpes, L. (1987) *J. Neurosci.* **7**, 1327–1339.
19. Florence, S. L., Conley, M. & Casagrande, V. A. (1986) *J. Comp. Neurol.* **243**, 234–248.
20. Hess, D. T. & Edwards, M. A. (1987) *J. Comp. Neurol.* **264**, 409–420.
21. Spatz, W. B., Illing, R. B. & Weisenhorn, D. M. (1994) *J. Comp. Neurol.* **339**, 519–534.
22. Dyck, R. H. & Cynader, M. S. (1993) *Proc. Natl. Acad. Sci. USA* **90**, 9066–9069.
23. Florence, S. L. & Kaas, J. H. (1992) *Visual Neurosci.* **8**, 449–462.
24. Fleagle, J. G. (1999) *Primate Adaptation and Evolution* (Academic, San Diego).
25. Horton, J. C. & Hedley-Whyte, E. T. (1984) *Philos. Trans. R. Soc. London B* **304**, 255–272.
26. Clarke, S. (1994) *Eur. J. Neurosci.* **6**, 725–736.
27. Jones, E., Hendry, S., DeFelipe, J. & Benson, D. (1994) in *Cerebral Cortex, Vol. 10: Primary Visual Cortex in Primates*, eds. Peters, A. & Rockland, K. (Plenum, New York), pp. 61–140.
28. Wong-Riley, M. T. T., Hevner, R. F., Cutlan, R., Earnest, M., Egan, R., Frost, J. & Nguyen, T. (1993) *Visual Neurosci.* **10**, 41–58.
29. Lund, J. S., Yoshioka, T. & Levitt, J. B. (1994) in *Cerebral Cortex, Volume 10: Primary Visual Cortex in Primates*, eds. Peters, A. & Rockland, K. (Plenum, New York), pp. 37–60.
30. Campbell, M. & Morrison, J. (1989) *J. Comp. Neurol.* **282**, 191–205.
31. Lee, V. M.-Y., Otvos, L., Jr., Carden, M. J., Hollosi, M., Dietzchold, B. & Lazzarini, R. A. (1988) *Proc. Natl. Acad. Sci. USA* **85**, 1998–2002.
32. Nimchinsky, E. A., Gilissen, E., Allman, J. M., Perl, D. P., Erwin, J. M. & Hof, P. R. (1999) *Proc. Natl. Acad. Sci. USA* **96**, 5268–5273.
33. Wong-Riley, M. (1979) *Brain Res.* **171**, 11–29.
34. Straus, W. (1982) *J. Histochem. Cytochem.* **30**, 491–493.
35. Preuss, T. M. & Kaas, J. H. (1996) *Brain Res.* **712**, 353–357.
36. Brodmann, K. (1909) *Vergleichende Lokalisationslehre der Grosshirnrinde* (Barth, Leipzig, Germany); trans. Garey, L. J. (1994) *Localisation in the Cerebral Cortex* (Smith-Gordon, London).
37. Lund, J. S. (1973) *J. Comp. Neurol.* **147**, 455–496.
38. Hässler, R. (1967) in *Evolution of the Forebrain*, eds. Hässler, R. & Stephan, H. (Thieme, Stuttgart), pp. 419–434.
39. Rogers, J. (1994) *Am. J. Phys. Anthropol.* **94**, 81–88.
40. Preuss, T. M., Qi, H.-X., Gaspar, P. & Kaas, J. H. (1997) *Soc. Neurosci. Abstr.* **23**, 1273.
41. Ang, L. C., Munoz, D. G., Shul, D. & George, D. H. (1991) *Brain Res. Dev. Brain Res.* **61**, 103–109.
42. Hof, P. R. & Morrison, J. H. (1995) *J. Comp. Neurol.* **352**, 161–186.
43. Hof, P. R., Ungerleider, L. G., Webster, M. J., Gattass, R., Adams, M. M., Sailstad, C. A. & Morrison, J. H. (1996) *J. Comp. Neurol.* **376**, 112–127.
44. Chaudhuri, A., Zangenehpour, S., Matsubara, J. & Cynader, M. (1996) *Brain Res.* **709**, 17–26.
45. Miklossy, J. (1992) in *The Functional Organization of Human Visual Cortex*, eds. Gulyas, B., Ohoson, D. & Rowland, P. E. (Pergamon, Oxford), pp. 123–136.
46. Tigges, J. & Tigges, M. (1979) *Brain Res.* **166**, 386–390.
47. Blasdel, G. G. & Fitzpatrick, D. (1984) *J. Neurosci.* **4**, 880–895.
48. Felleman, D. J. & Van Essen, D. C. (1991) *Cereb. Cortex* **1**, 1–47.
49. Tootell, R. B., Mendola, J. D., Hadjikhani, N. K., Ledden, P. J., Liu, A. K., Reppas, J. B., Sereno, M. I. & Dale, A. M. (1997) *J. Neurosci.* **17**, 7060–7078.
50. Livingstone, M. S., Rosen, G. D., Drislane, F. W. & Galaburda, A. M. (1991) *Proc. Natl. Acad. Sci. USA* **88**, 7943–7947.
51. Demb, J. B., Boynton, G. M. & Heeger, D. J. (1998) *J. Neurosci.* **18**, 6939–6951.
52. Crick, F. & Jones, E. G. (1993) *Nature (London)* **361**, 109–110.
53. Preuss, T. M. (1999) in *The New Cognitive Neurosciences*, ed. Gazzaniga, M. S. (MIT Press, Cambridge, MA), in press.
54. Preuss, T. M. & Kaas, J. H. (1999) in *Fundamental Neuroscience*, eds. Bloom, F. E., Landis, S. C., Robert, J. L., Squire, L. R. & Zigmond, M. J. (Academic, San Diego), pp. 1283–1311.
55. Jerison, H. J. (1973) *Evolution of the Brain and Intelligence* (Academic, New York).
56. Blümcke, I., Hof, P. R., Morrison, J. H. & Celio, M. R. (1990) *J. Comp. Neurol.* **301**, 417–432.
57. del Río, M. R. & DeFelipe, J. (1997) *J. Chem. Neuroanat.* **12**, 165–173.
58. Hendry, S. H. & Carder, R. K. (1993) *Visual Neurosci.* **10**, 1109–1120.
59. Tootell, R. B. & Taylor, J. B. (1995) *Cereb. Cortex* **5**, 39–55.